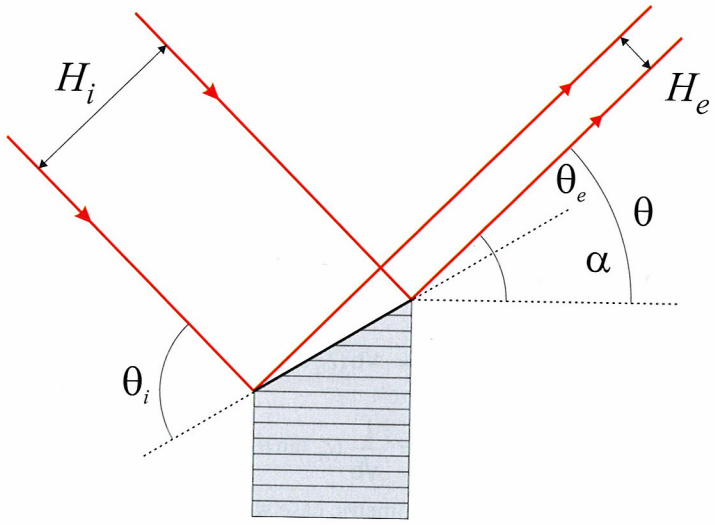

Fig. 6.11 Asymmetric Bragg reflection. The surface of the crystal is at an angle α with respect to the reflecting atomic planes. The widths of the incident and scattered beams are then different. In this case the parameter b is greater than one.

bandwidth ζ (which is proportional to x from Eq. (6.45)) is independent of energy, the angular Darwin width is not.

In Fig. 6.10(c) we provide an example of how the Darwin width depends on the polarization of the incident beam. Up until now we have mostly assumed that the incident beam is polarized perpendicular to the scattering plane, so-called $\hat{\sigma}$ polarization, see Fig. 2.5, for which the polarization factor $P = 1$. With the polarization in the scattering plane – $\hat{\pi}$ polarization – the scattering amplitude is reduced by a factor of $\cos(2\theta)$. In this latter case the primary beam therefore penetrates more deeply into the crystal producing a narrower Darwin width, as evidenced in Fig. 6.10(c). Another way of describing the polarization dependence of the reflectivity curve is to say that in the tails of the Darwin curve perfect crystals are birefringent, i.e. they exhibit a difference in the refractive index for waves polarized in orthogonal directions. This birefringence allows the construction of X-ray phase plates for manipulating the polarization of the beam. For example, a quarter-wave plate can be used to convert the polarization from linear to circular.

6.4.7 Asymmetric Bragg geometry

In general the surface of a crystal will not be parallel to the atomic planes which reflect the incident beam, as shown in Fig. 6.11. Let α be the angle between the surface and the reflecting planes. The incident, θ_i, and exit, θ_e, glancing angles are then given by $\theta_i = \theta + \alpha$ and $\theta_e = \theta - \alpha$. For a reflection geometry it is required that both θ_e and θ_i are greater than zero, or in other words that α fulfils the condition $0 < |\alpha| < \theta$. In Fig. 6.11 α has been chosen to be greater than zero. This implies a compression of the width of the exit beam. The asymmetry parameter, b, is defined by

$$\mathsf{b} \equiv \frac{\sin\theta_i}{\sin\theta_e} = \frac{\sin(\theta+\alpha)}{\sin(\theta-\alpha)} \tag{6.46}$$

Symmetric Bragg diffraction corresponds to setting $b = 1$. For the particular case shown in the Fig. 6.11, $b > 1$. The widths of the incident, H_i, and exit, H_e, beams are related by the equation

$$H_i = b\, H_e$$

It turns out that a compression in the width of the exit beam implies an increase in its angular divergence. This is a consequence of Liouville's theorem[7]. By the same reasoning the acceptance angle of the incident beam must decrease to compensate for the increase in the incident beam width. Let the angular acceptance of the incident beam be $\delta\theta_i$, and the reflected beam divergence be $\delta\theta_e$. We now assert that $\delta\theta_i$ and $\delta\theta_e$ are given in terms of the asymmetry parameter b and the Darwin width ζ_D by the equations

$$\delta\theta_e = \sqrt{b}\,(\zeta_D \tan\theta) \tag{6.47}$$

and

$$\delta\theta_i = \frac{1}{\sqrt{b}}\,(\zeta_D \tan\theta) \tag{6.48}$$

These formulae are certainly correct in the symmetric case with $b = 1$ (see Eq. (6.28)). Moreover, since

$$\delta\theta_i\, H_i = \frac{1}{\sqrt{b}}\,(\zeta_D \tan\theta)\; bH_e = \sqrt{b}\,(\zeta_D \tan\theta)\; H_e = \delta\theta_e\, H_e$$

the product of beam width and divergence is the same for the incident and exit beams, as required by Liouville's theorem.

An interesting application of asymmetric crystals is in the measurement of Darwin reflectivity curves. The angular Darwin width is small, typically of order of ~0.002°, c.f. Fig. 6.10. Measurement of the reflectivity curve then requires a detector system that has a much better angular resolution than this value. This follows from the fact that the measured curve is the *convolution* of the Darwin reflectivity curve of the crystal and the angular resolution of the detector, or analyser, system. So if the angular divergence of the analyser is much smaller than that of the first crystal, then the measured curve is determined solely by the Darwin reflectivity of the first crystal. One way to achieve high angular resolution in the analyser is to use an asymmetric crystal. From Eq. (6.47), its angular acceptance can be made arbitrarily small by decreasing the value of b. Double crystal spectrometers with two perfect crystals are discussed further in the next section on DuMond diagrams.

In Fig. 6.12 we show data from a double crystal diffractometer composed of two perfect asymmetric silicon crystals. With two asymmetric crystals there are four possible ways of configuring the diffractometer. The narrowest curve is recorded when the first crystal is arranged with $b<1$, and the second with $b>1$. In this case the diffracted beam from the first crystal has the smallest possible angular divergence, which is matched to the narrow angular acceptance of the second.

6.5 DuMond diagrams

An optical element inserted into an X-ray beam is supposed to modify some property of the beam such as its width, its divergence, or its wavelength band. It is useful to describe the modification of the beam by a transfer function. The transfer function relates the input parameters of the beam upstream from the optical element to the output parameters of the beam after the beam has passed the optical element.

[7] Liouville's theorem states that for beams of particles, here photons, the product of beam width and divergence is a constant.

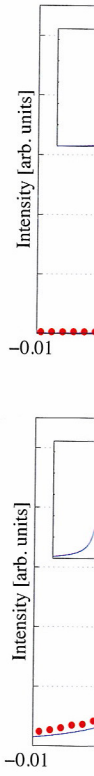

Fig. 6.12 Measu
solid lines represe
were configured.

When the c
the beam diver
the transfer fu
to the left and
normalized by
Darwin curve
the $(\theta_i, \lambda/2d)$ p
within an angu
given by $\lambda/2d$

One crystal

According to E
if the angle of i

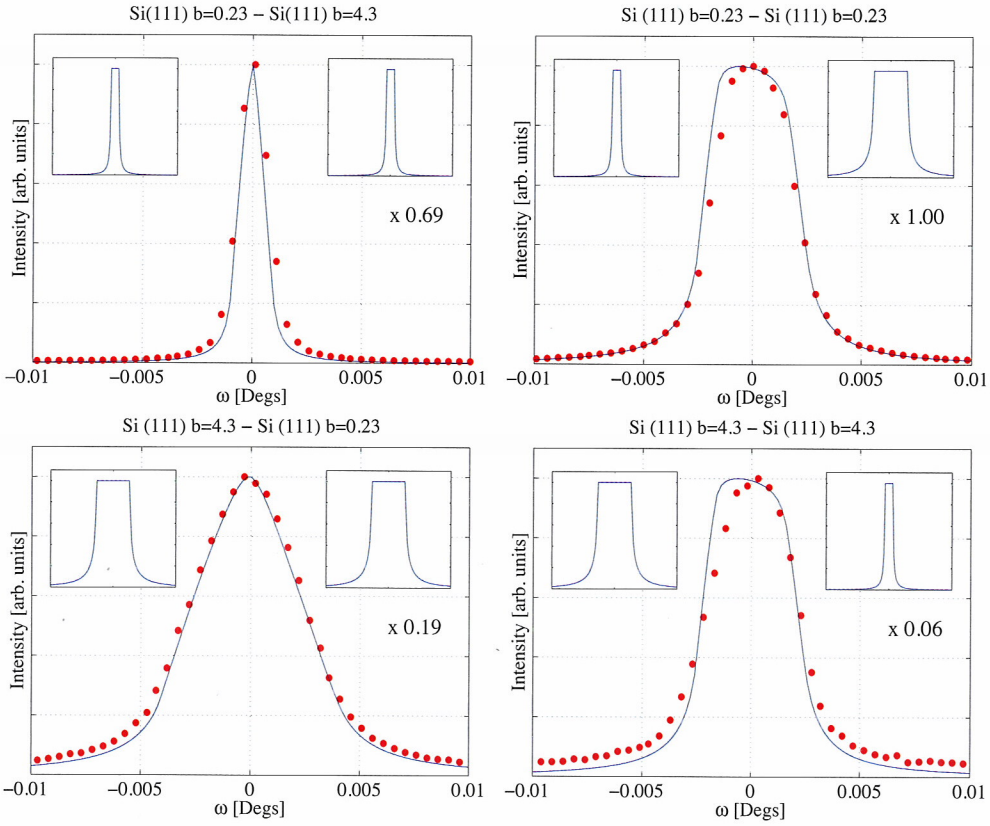

Fig. 6.12 Measured rocking curves for a double crystal diffractometer formed from two asymmetric perfect silicon crystals. The solid lines represent the calculated convolution of two Darwin curves with widths determined by how the asymmetric crystals were configured.

When the optical element is a perfect crystal the relevant beam parameters are amongst other things the beam divergence and the wavelength band. The DuMond diagram is a graphical representation of the transfer function. In the diagram the horizontal axes are the beam divergence, with the input beam to the left and the output beam to the right. The vertical axis is common and is $\lambda/2d$, the wavelength normalized by twice the lattice spacing d. In the crudest approximation, where the finite width of the Darwin curve and refraction effects are neglected, only the points of the incident parameter space in the $(\theta_i, \lambda/2d)$ plane which satisfy $\lambda/2d = \sin\theta_i$ will be reflected. For a white incident beam that falls within an angular window $\theta_{i,\min} < \theta_i < \theta_{i,\max}$ the output side of the DuMond diagram consists of a line given by $\lambda/2d = \sin\theta_e$ with $\theta_{i,\min} < \theta_e < \theta_{i,\max}$.

One crystal

According to Bragg's law, constructive interference of waves scattered from an infinite crystal occurs if the angle of incidence, θ_B, and the wavelength, λ, are related exactly by

$$m\lambda = 2d\sin\theta_B$$

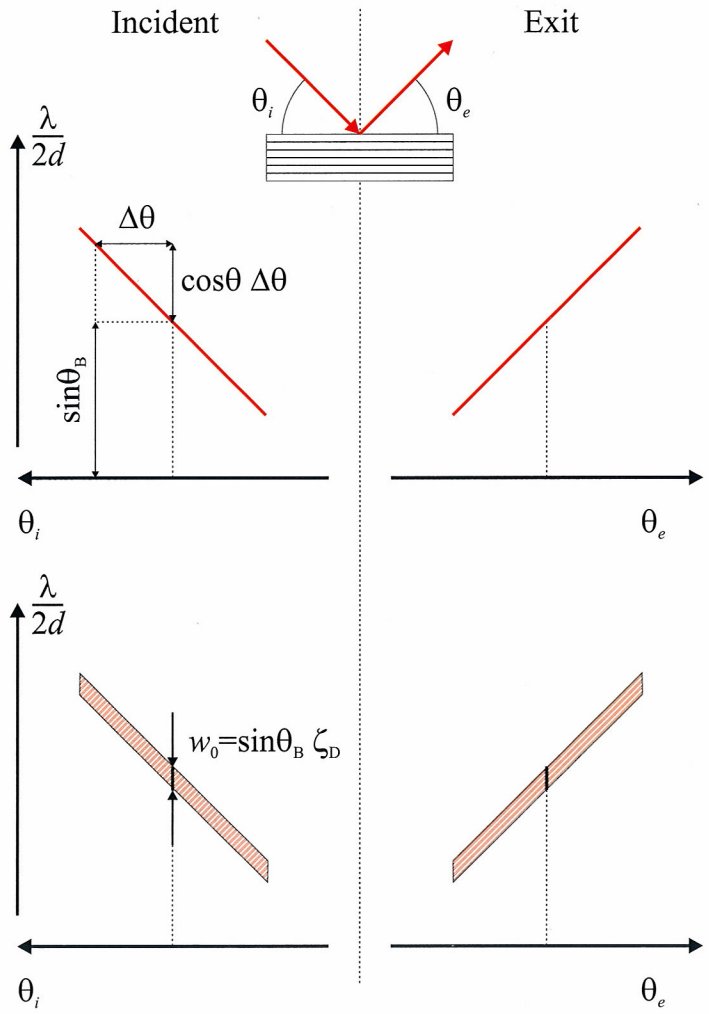

Fig. 6.13 DuMond diagram for symmetric Bragg geometry. In this case the angles of the incident, θ_i, and exit, θ_e, beams relative to the crystal surface are the same. The DuMond diagram is a graphical representation of the Bragg reflection condition, where the axes are angle, relative to the Bragg angle θ_B, and $\lambda/2d$. In (a) the Darwin width has been neglected. The intensity is non-zero for points on the line only. (b) The finite Darwin width broadens the line into a band with a width along the ordinate of $w_0 = \sin\theta_B \zeta_D$.

One way to represent this relationship is to plot a graph with $\lambda/2d$ on the ordinate and θ_B on the abscissa. Any point on the sinusoidal curve gives values of $\lambda/2d$ and θ_B that satisfy Bragg's law. Perfect crystals diffract over a small but finite range in angle and wavelength. When dealing with perfect crystals it is therefore necessary to consider deviations of the incident angle θ_i around θ_B, and deviations of wavelength around the value given by $2d \sin\theta_B$. For asymmetric crystals it is also necessary to consider the exit angle θ_e of the reflected beam.

The DuMond diagram is a graphical way to represent diffraction events, and is composed of two parts: one is a plot of $\lambda/2d$ against $\theta_i - \theta_B$, with θ_i increasing to the left; and the other is a plot of $\lambda/2d$ against $\theta_e - \theta_B$, with θ_e increasing to the right. For small deviations away from the Bragg condition

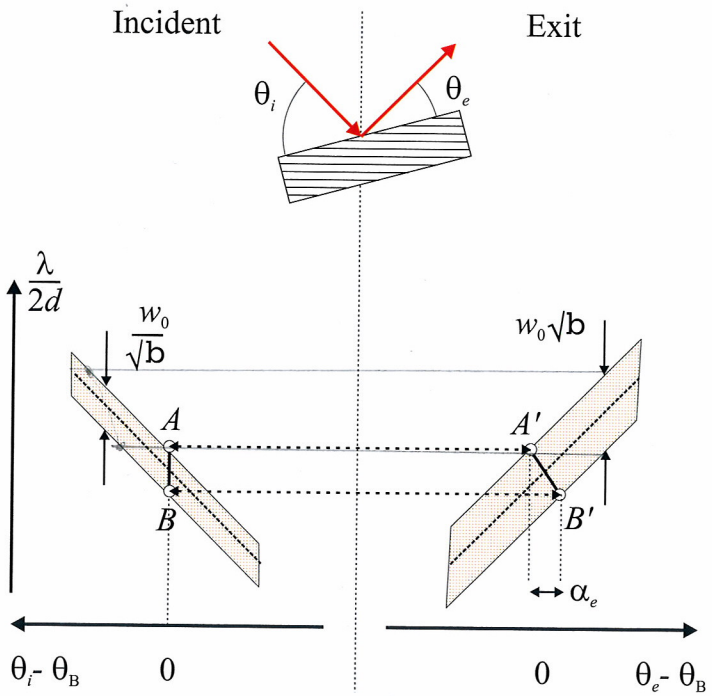

Fig. 6.14 DuMond diagram for asymmetric Bragg geometry. The ratio of the widths of the incident and exit beams is given by the parameter b. This implies that the angular acceptance of the incident beam is reduced by a factor of $1/\sqrt{b}$ while that of the exit beam is increased by the same amount. Thus in the DuMond diagram the incident bandwidth is reduced, and the exit one increased. Points A and B on the incident side are associated with points A' and B' on the exit side. This shows that an incident beam which is parallel and white acquires a finite angular divergence given by α_e when it has been diffracted by a crystal set in asymmetric Bragg geometry.

the sinusoidal dependence of $\lambda/2d$ approximates to a straight line with slope $\cos\theta$. The top part of Fig. 6.13 shows the DuMond diagram for a crystal diffracting according to Bragg's law in a symmetric reflection geometry. When neglecting the finite Darwin width, the reflectivity is non-vanishing only on the line indicated, and the relative change in wavelength $\Delta\lambda/\lambda$ and the deviation $\Delta\theta$ from the Bragg angle are related by

$$\frac{\Delta\lambda}{\lambda} = \frac{\Delta\theta}{\tan\theta}$$

For the symmetric Bragg geometry assumed here the surface coincides with the reflecting planes: the reflection is specular, and the wavelength and exit angle are linked by the same condition as the one above.

The lower part of Fig. 6.13 shows the DuMond diagram for symmetric Bragg geometry, but now including the finite Darwin bandwidth: all wavelengths from a perfectly collimated white source within a relative bandwidth ζ_D have a reflectivity of 100%. Outside of this band, the reflectivity falls off quickly as we move from the dynamical to the kinematical regimes (see Fig. 6.3 and 6.5). In the latter the scattering is located along the crystal truncation rods which run parallel to the surface normal (Section 5.3). In terms of the DuMond ordinate $\lambda/2d$ the width of the central band is

$$w_0 = \frac{\Delta\lambda}{2d} = \left(\frac{\lambda}{2d}\right)\left(\frac{\Delta\lambda}{\lambda}\right) = \left(\frac{\lambda}{2d}\right)\zeta_D = \sin\theta_B\,\zeta_D \qquad (6.49)$$

where $\zeta_D = \Delta\lambda/\lambda$ is the Darwin width given by Eq. (6.25). As indicated, symmetry implies that a perfectly collimated incident beam is reflected to a perfectly collimated exit beam.

This is not the case for an asymmetric crystal, where the surface does not coincide with the reflecting planes, as is shown in Fig. 6.14. The exit beam width is now smaller than that of the incident beam. In Section 6.4.7 it has been shown that this implies that the bandwidth of the incident beam is reduced by a factor of $1/\sqrt{b}$, while the bandwidth of the exit beam is increased by a factor of $\sqrt{b}$. It is important to note that the crystal truncation rod is no longer parallel to the reciprocal lattice vector, since it runs perpendicular to the surface. The consequences of these considerations are illustrated in the lower part of Fig. 6.14. A perfectly collimated incident beam is reflected in the band AB. The scattering is elastic, so the point $A(B)$ is transferred to point $A'(B')$ on the exit part of the DuMond diagram. Since the points A' and B' have different abscissa, displaced by the amount α_e, a perfectly collimated incident beam acquires a finite divergence after Bragg reflection.

In the examples of the symmetric and asymmetric Bragg geometries there is an ambiguity left to resolve. This concerns the question of how to relate points on the DuMond diagram of the incident beam with those of the exit beam. For the asymmetric Bragg case, shown in the lower part Fig. 6.14, the point A on top of the incident band is shown connected to the point A' on top of the exit band. (The line runs at right angles to the $\lambda/2d$ axis since the scattering is elastic.) The reason for this is illustrated in Fig. 6.15, which should be compared with Fig. 6.1. The transition from the dynamical to the kinematical regimes must be continuous. In the kinematical regime the scattering lies along the crystal truncation rods (CTR's). If the incident beam is white and parallel then the crystal reflects a band Δk out of the incident beam. A given wavevector in the incident beam, $\mathbf{k}_1$ say, is scattered to a final wavevector $\mathbf{k}'_1$, with $|\mathbf{k}_1| = |\mathbf{k}'_1|$. The direction of $\mathbf{k}'_1$ is found from where the Ewald sphere, indicated by the circular arc, crosses the CTR. For the asymmetric Bragg case the truncation rod does not lie along the direction of the wavevector transfer: it runs perpendicular to the physical surface. From Fig. 6.15(b) this implies that the scattering angle of the exit beam must increase as $|\mathbf{k}'|$ increases. This is consistent with the choice of associating B with B'. Continuity between the dynamical and kinematical regime also implies that the central band of the former does not lie along the wavevector transfer. In other words the reflection is not specular.

The same construction is shown for symmetric Laue geometry in Fig. 6.15(c). From this it is clear that a crystal diffracting in symmetric Laue geometry will impart a finite angular divergence to a parallel, white incident beam.

Two crystals in symmetric Bragg geometry

In Fig. 6.16 a white beam is incident on a crystal at a certain Bragg angle. To simplify the discussion it is assumed, as in the previous section, that the Darwin reflectivity curve may be approximated by a box function. The beam incident on the first crystal is thus the vertical, light shaded band with an angular width $2\Delta\theta_{in}$ in the DuMond diagrams in the lower part of the figure. A second crystal is set to reflect the central ray. This can be done in two ways.

If the Bragg planes in the second crystal are parallel to those in the first crystal, a ray deviating (dotted line) from the central ray by $\Delta\theta_{in}$ will be reflected at the same setting as the central ray. In a DuMond diagram this means that the response band of the second crystal is parallel to that of the first crystal. In scanning the angle of the second crystal there is no overlap with the intensity provided by the first crystal for any of the four settings shown. Only when the angular setting of the second crystal is in between those labelled 2 and 3 will there be scattered intensity after the second crystal. Since the bands are assumed to be box-like, the intensity versus angle will be triangular with a FWHM equal to the angular Darwin width w_1 of one crystal, independent of the incident angular bandwidth.

(a)

Δk

(b)

Δk

(c)

Δk

Fig. 6.15 Scatterin
symmetric Laue geo
with the darker shade
points A, B and A', B'
way.

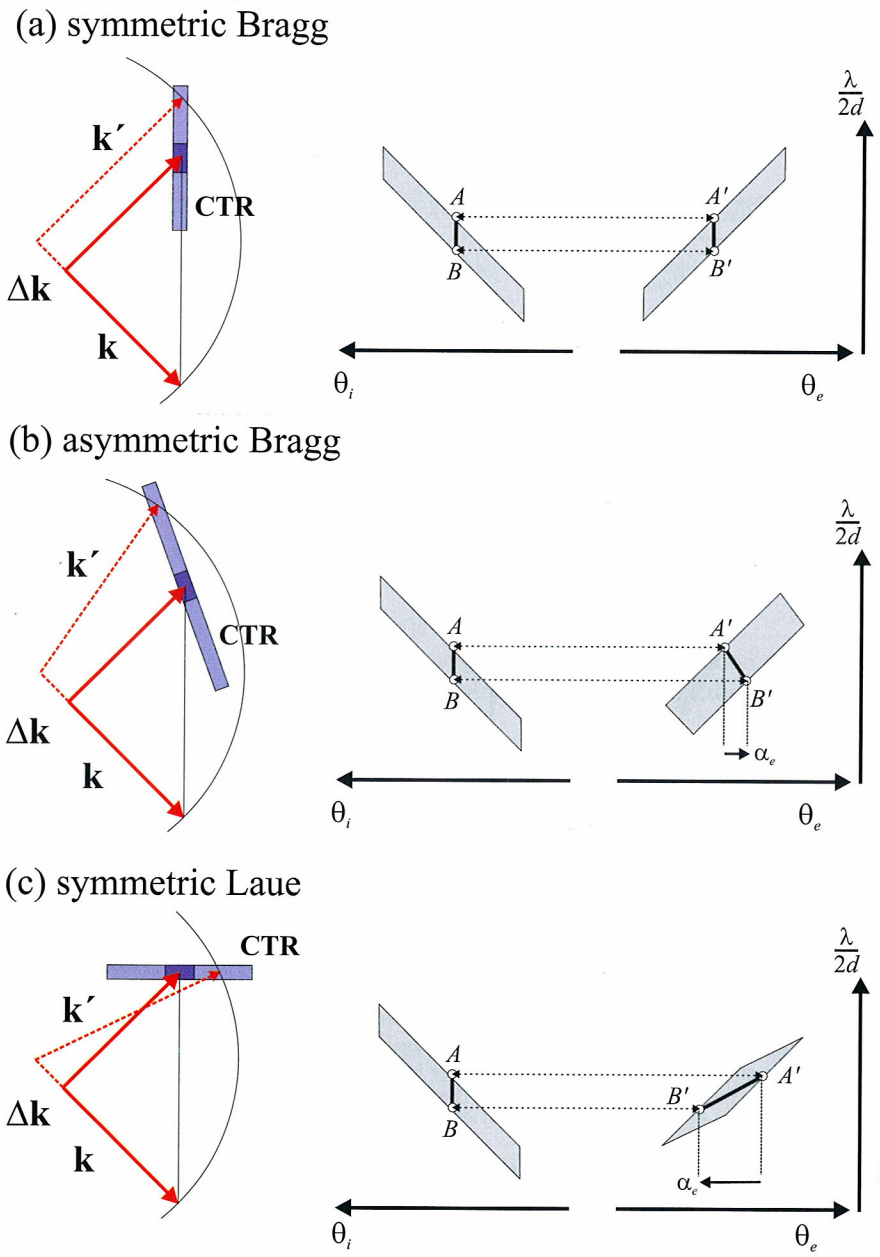

Fig. 6.15 Scattering triangles (left) and DuMond diagrams (right) for (a) symmetric Bragg, (b) asymmetric Bragg and (c) symmetric Laue geometries. In the scattering triangles the crystal truncation rod (CTR) is represented by the rectangular box, with the darker shaded part being the central dynamical band. Continuity between the kinematical and dynamical regimes allows points A, B and A', B' in the DuMond diagrams of the incident and exit beams to be associated with each other in an unambiguous way.

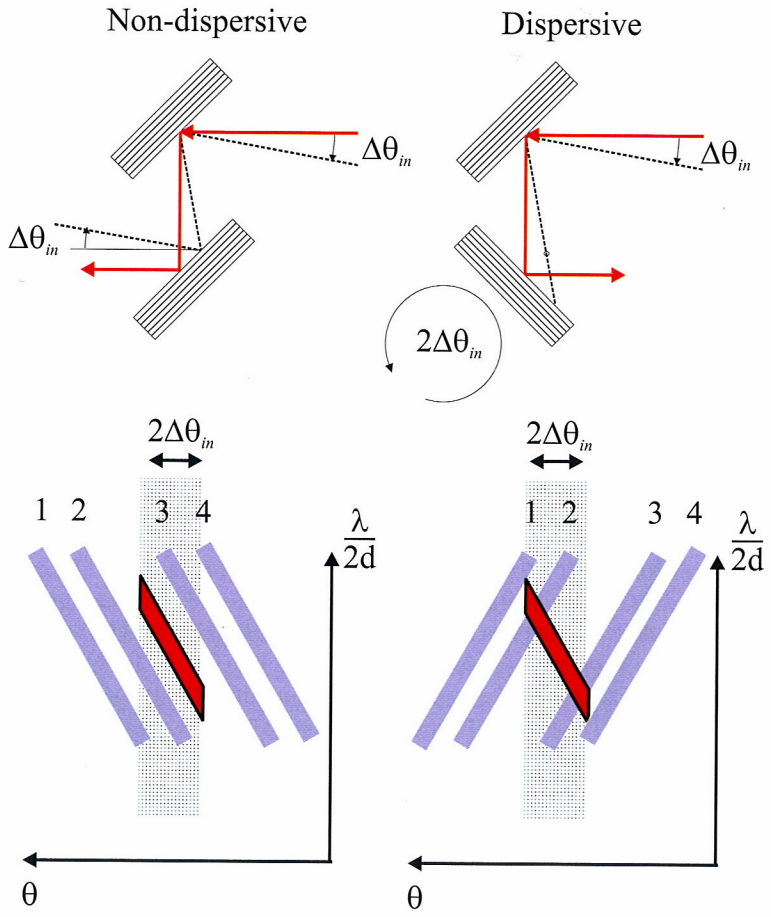

Fig. 6.16 Non-dispersive geometry (left): X-rays from a white source are incident on two crystals aligned in the same orientation. The central ray (full line) will be Bragg reflected by both crystals and will emerge parallel to the original ray. A ray incident at a higher angle than that of the central ray will only be Bragg reflected if it has a longer wavelength. The angle of incidence this ray makes with the second crystal is the same as that it made with the first, and will be Bragg reflected. The DuMond diagram in the lower part shows that a scan of the second crystal has a width equal to the convolution of the Darwin widths of the two crystals, independent of the incident angular divergence. Dispersive geometry (right): A ray incident at a higher angle than the central ray at the first crystal will be incident at a lower angle at the second crystal. The second crystal must be rotated by the amount $2\Delta\theta_{in}$ for Bragg's law to be fulfilled. The geometry is therefore wavelength dispersive.

Furthermore, the reflected wavelength band from the second crystal equals that after the first crystal and is determined by the angular spread $2\Delta\theta_{in}$. This orientation is therefore termed non-dispersive.

On the other hand, in the alternative orientation, the response band of the second crystal has the opposite slope to that of the first crystal. The angular width is now dependent of the incident width: in the limit of a very small Darwin width w_1 it is actually equal to that of the incident width. In the DuMond diagram there will be scattering after the second crystal in all of the positions 2 through 4. The wavelength bandwidth after the second crystal in position 3 is now much smaller than the wavelength bandwidth after the first crystal, and the orientation is termed dispersive. It is clear that this qualitative discussion of the dispersive setting can be sharpened to a quantitative estimate of both the angular and